#### **NURETH14-460**

# THERMAL-HYDRAULICS AND NEUTRONICS STUDIES ON THE FP7 CP-ESFR OXIDE AND CARBIDE CORES

## L. Ammirabile<sup>1</sup> and H. Tsige-Tamirat<sup>1</sup>

<sup>1</sup> European Commission, JRC, Institute for Energy, Petten, The Netherlands

#### **Abstract**

In the framework of the Collaborative Project on European Sodium Fast Reactor (CP-ESFR) two core designs that are currently being proposed for the 3600 MWth sodium-cooled reactor concept: one is based on oxide fuel and the other on carbide fuel.

Using the European Safety Assessment Platform (ESAP), JRC-IE has conducted static calculation on neutronics (incl. reactivity coefficients) and thermal-hydraulic characteristics for both oxide and carbide reference cores. The quantities evaluated include: keff, coolant heat-up, void, and Doppler reactivity coefficients, axial and radial expansion reactivity coefficients, pin-by-pin calculated power profiles, average and peak channel temperatures. This paper presents the ESAP models applied in the study together with the relevant results for the oxide and carbide core.

#### Introduction

Fast Reactors have a unique capability as sustainable energy source; the closed fuel cycle allows significantly improving the usage of natural resources and the minimisation of volume and heat load of high-level waste. Among the fast reactor systems, the sodium-cooled fast reactor has the most comprehensive technological basis, thanks to the experience gained internationally from operating experimental, prototype and commercial size reactors. Therefore, a proposal for a large integrated Collaborative Project on European Sodium Fast Reactor (CP ESFR) was proposed to be realized under the aegis of the 7th FP to answer the EURATOM Work programme 2008 [1].

In frame of the ESFR project two core designs are currently being proposed for the 3600 MWth sodium-cooled reactor concept: the first is based on the oxide fuel and the second on the carbide fuel. Starting from these 'working horses' cores, different options will be proposed and evaluated within the ESFR project with respect to the following goals:

- Enhancement of nominal core performances (average discharged burn-up, plutonium mass to be loaded, cycle length etc.)
- Enhancement of the core safety by means of reduction of the sodium void coefficient and/or optimization leading to gain significant margins on the behaviour of these cores in the frame of unprotected transients.

This paper focuses mainly on the open fuel cycle neutronic and thermal-hydraulic analyses for the basic oxide and carbide working horse cores.

#### 1. ESFR core geometries

In this study the numerical codes were applied to the ESFR working horses. The cores geometry is

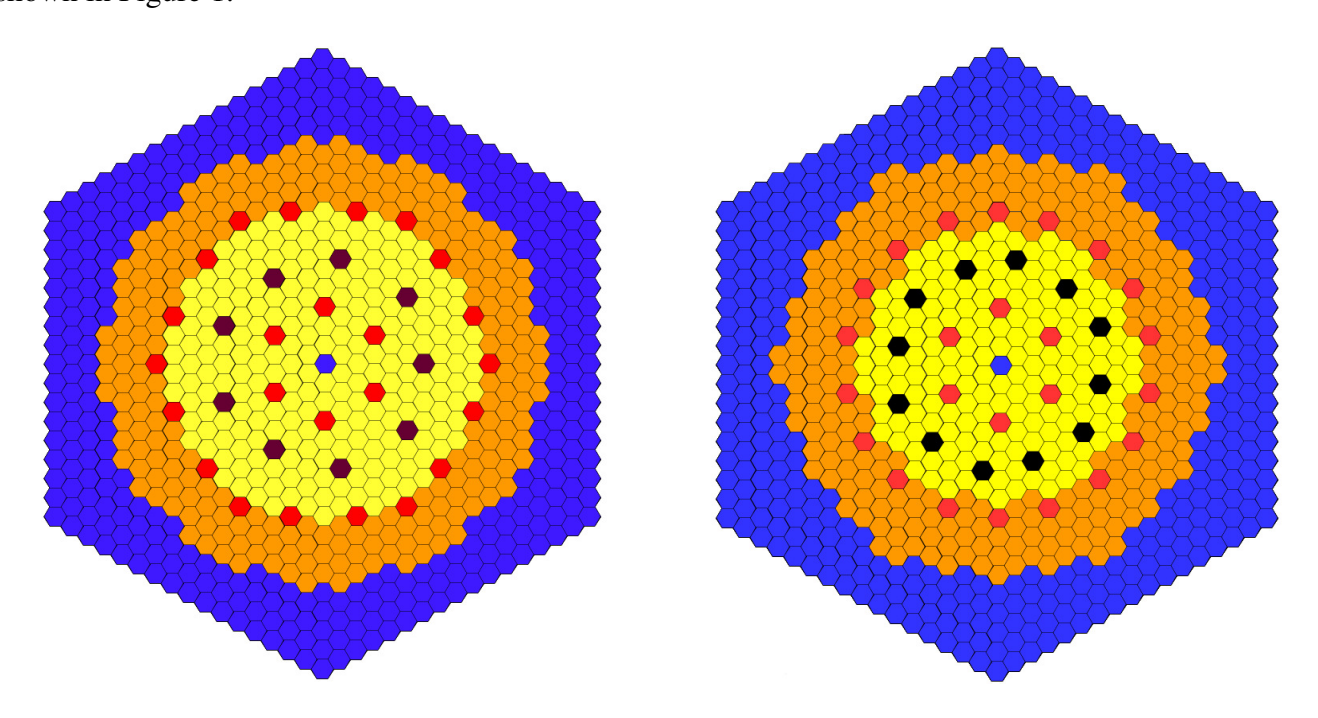


Figure 1 Cross-section of the oxide (left) and carbide (right) ESFR.

The ESFR core is flat to provide good thermal-hydraulic properties and to enhance the leakage, which improves the sodium void effect. The main reactor parameters are summarized in Table 1. The core is characterized by large power density and in-pile fuel mass. The carbide core has lower volume and loaded mass of actinides, but it provides higher burn-up during shorter residence time. It has also higher relative but lower absolute Pu content.

ESFR core version	oxide	carbide
Thermal power	3600 MW <sub>th</sub>	3600 MW <sub>th</sub>
Volume	$17.5 \text{ m}^3$	$10.5 \text{ m}^3$
Lattice pitch	20.08 cm	18.32 cm
Fuel type	Pins / Pellets	Pins / Pellets
Nr. of fuel assemblies	453	414
Diameter	4.72 m	4.10 m
Height	1.00 m	0.80 m
H/D ration	0.21	0.19
Actinides	74.1 tons	39.5 tons
Plutonium	11.6 tons (15.7%)	8.5 tons (21.5%)
Core management	5 x 410 = 2050	3 x 533 = 1600
	EFPD	EFPD
Average burn-up	~10 % FIMA	~15 % FIMA
	~100 GWd/tHM	~150 GWd/tHM
Inlet coolant temp.	395 °C	395 °C
Outlet coolant temp.	545 °C	545 °C

Table 1 ESFR core parameters

## 2. European Safety Assessment Platform (ESAP)

The ESAP (European Safety Analysis Platform) is a computational platform that has the objective to perform an integrated core and safety analysis of nuclear reactor systems. The platform is based on existing well-qualified nuclear codes: MCNP5 for neutron transport calculations, COBRA for core and sub-channel analysis and FRETA-B for fuel thermal-mechanical behaviour studies. The ESAP platform is currently under development. The final structure of ESAP will consist of a static safety core analysis section, a fuel cycle analysis section and a dynamic safety system analysis section as shown in Figure 2.

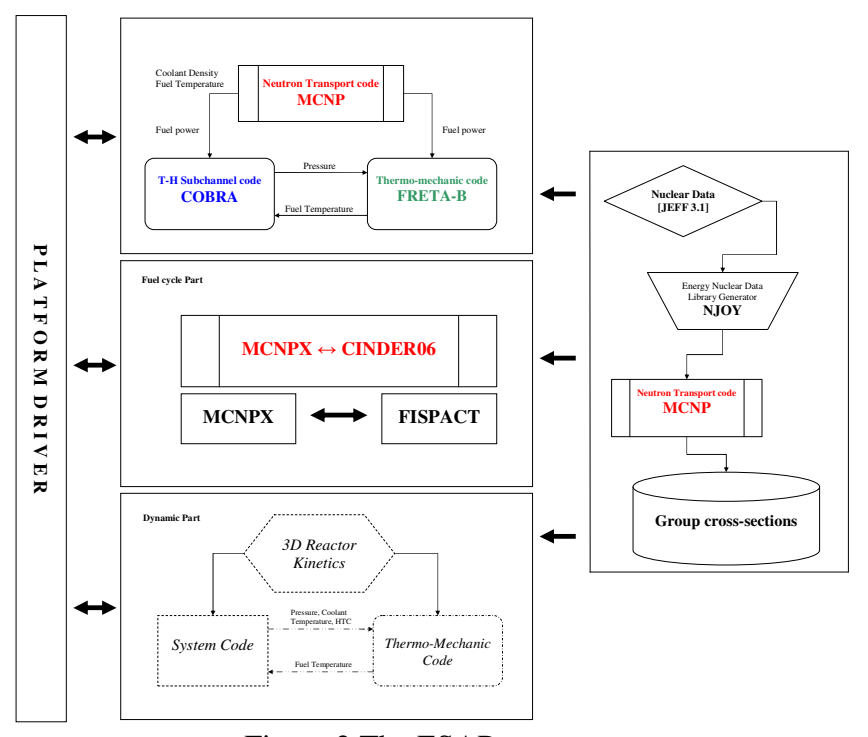


Figure 2 The ESAP structure.

The static and fuel cycle part of ESAP are instead fully operational tools. The methodology used in ESAP for static fast reactor design analysis is based upon Monte Carlo method for neutronics and subchannel code for thermal hydraulics. This approach provides several advantages such as a full three dimension treatment of the problem geometry, the use of continuous energy cross sections and subchannel geometry for thermal-hydraulics.

On the other hand, the computational and modelling effort for the Monte Carlo method is higher than for most deterministic methods. The static core analysis section of ESAP is based on the nuclear data processing code NJOY [2] for generation of temperature dependent continuous energy cross section library, the Monte Carlo transport codes MCNP/MCNPX [3],[4] for neutronics calculations, the subchannel thermal-hydraulics code COBRA-IV-I [5] and the thermo-mechanic fuel code FRETA-B [6] supplemented by several pre/post processing codes.

Basic nuclear data are taken from the Joint Evaluated Fission and Fusion File (JEFF-3.1). Temperature dependent, continuous energy nuclear data libraries based on JEFF-3.1 library were generated using the nuclear data processing code NJOY.

The Monte Carlo particle transport codes MCNP and MCNPX developed at Los Alamos National Laboratory are used for all neutron transport, criticality, and burnup calculations. Both MCNP and MCNPX perform stochastic neutron transport and criticality calculations in a fully resolved three-dimension full core geometry using continuous energy cross sections. The geometry modelling in MCNP/MCNPX is based on combinatorial geometry where a geometrical structure can be repeated to generate more complex systems. The use of the repeated structure feature allows efficient core geometry set up. Burnup calculations were performed using MCNPX which is internally coupled with the depletion code CINDER90 [7]. MCNPX provides to the CINDER90 code reaction rates for major isotopes possessing transport cross sections and neutron spectra in 63 energy groups for each burnup zone. CINDER90 generates effective cross sections by collapsing the 63 group cross section with the provided neutron spectra and performs then the depletion calculation for the burnup interval assuming constant flux over the interval. It returns back to MCNPX the nuclide inventories at the end of the burnup interval. The nuclide inventories are calculated using the predictor/corrector method which requires two criticality calculations per burnup interval for prediction and correction steps.

The COBRA-IV-I code belongs to the series of the COBRA (COolant Boiling in Rod Arrays) subchannel analysis computer programs which were originally developed by Pacific Northwest Laboratories (PNL). It is an extended version of the COBRA-IIIC subchannel analysis code which computes the flow and enthalpy distributions in nuclear fuel rod bundles or cores for both steady state and transient conditions.

The FRETA-B (Fuel Reliability Evaluation Code for Transients and Accidents – Bundle Geometry) is a computer code for analyzing the behaviour of fuel rods for nuclear reactors in nominal and accidental conditions.

The heat conduction equation is solved by the method of weighted residuals and includes the Ross-Stoute model [8] for gap conductance as well as a fuel relocation model.

The use of FRETA-B code is targeted to compute the fuel rod temperature profiles.

#### 2.1 MCNP modeling

Using the core compositions and the geometry specification of the ESFR, a detailed three-dimensional MCNP model for the oxide and carbide ESFR cores have been setup. The models reproduce the geometry fully resolved in radial and axial direction as given in the design specification. The repeated structure feature of MCNP has been used to set up the geometry model of the subassemblies and the full core models (Figure 3).

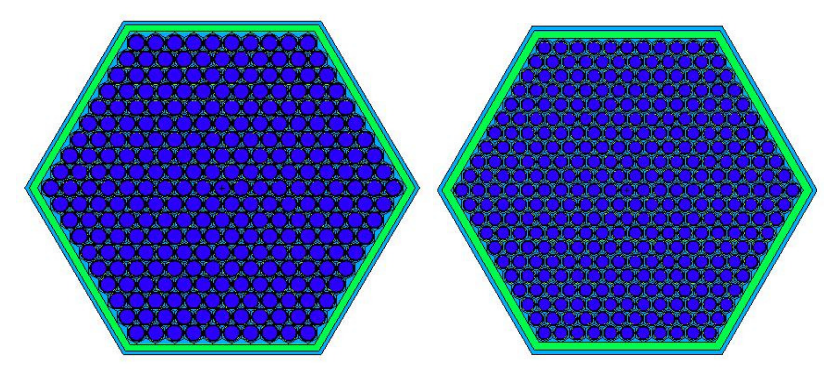


Figure 3 MCNP model of the oxide and carbide ESFR assemblies.

Figure 4 shows horizontal and vertical cuts of the three-dimensional full core geometry MCNP model of the oxide and carbide ESFR core. The different colours represent the radial reflectors, inner and outer fuel sub-assemblies, and the Control and Shutdown device (CSD) and the Diverse Shutdown Device (DSD) sub-assemblies. The vertical cuts depict the different axial regions including the lower and upper blankets and gas plena. Further, refinements of the models were performed for the burnup and power distribution calculations.

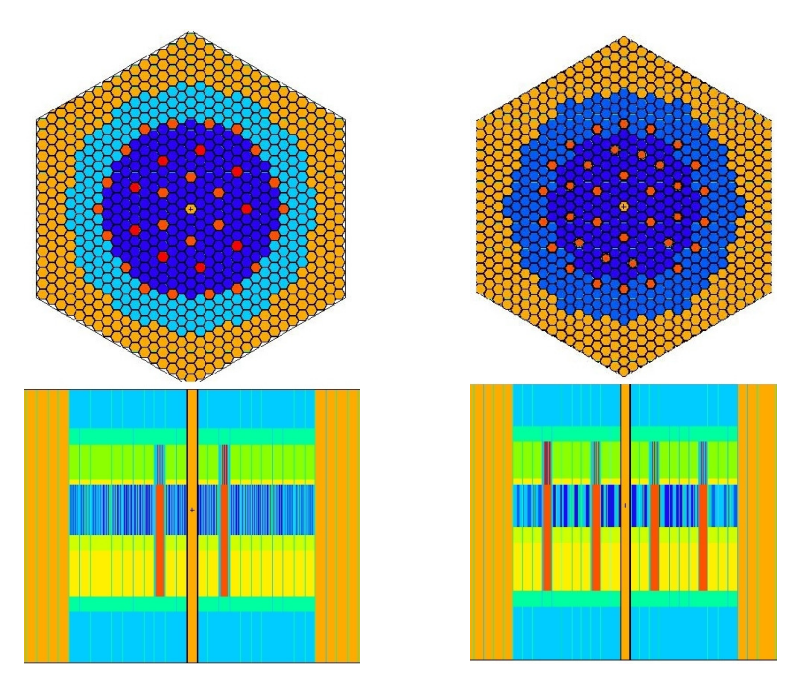


Figure 4 Horizontal and vertical cuts of the MCNP oxide and carbide core model of ESFR.

## 2.2 COBRA Modelling

With reference to the core geometry of ESFR and in full agreement with MCNP models a detailed 3D COBRA-IV-I model for oxide and carbide ESFR cores have been setup. The model represents the geometry fully resolved in radial and axial direction as given in the design specification. Based on the geometry data, a COBRA model for the oxide and carbide fuel assembly was prepared.

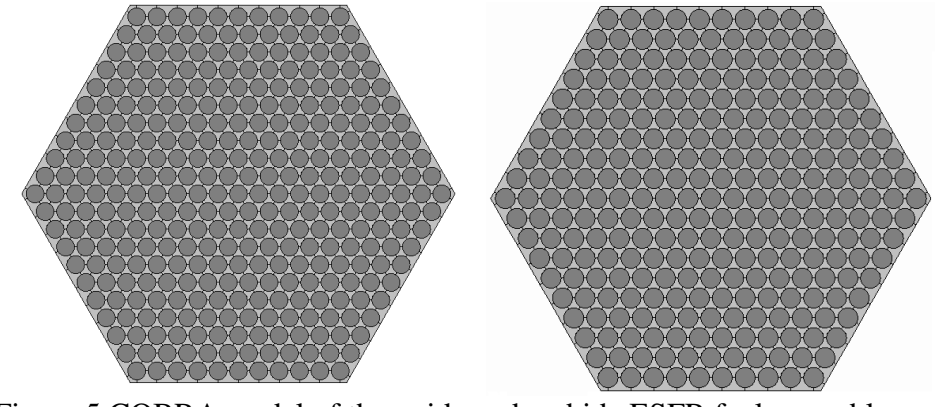


Figure 5 COBRA model of the oxide and carbide ESFR fuel assembly.

The oxide model consists of 546 sub-assembly channels that surround the 271 fuel pins. The carbide model consists of 666 sub-assembly channels that surround 331 fuel pins. The wire-wrap model is included. Both assemblies are divided vertically into 30 axial nodes. Figure 5 shows the cross-sections of oxide and carbide fuel assembly.

The cross-sections of COBRA full core geometry model of the oxide and carbide ESFR core is depicted in Figure 6. The COBRA model consists of parallel assembly channels that include the inner core region, the outer core region, and the control assemblies. The core is divided vertically into 30 axial nodes.

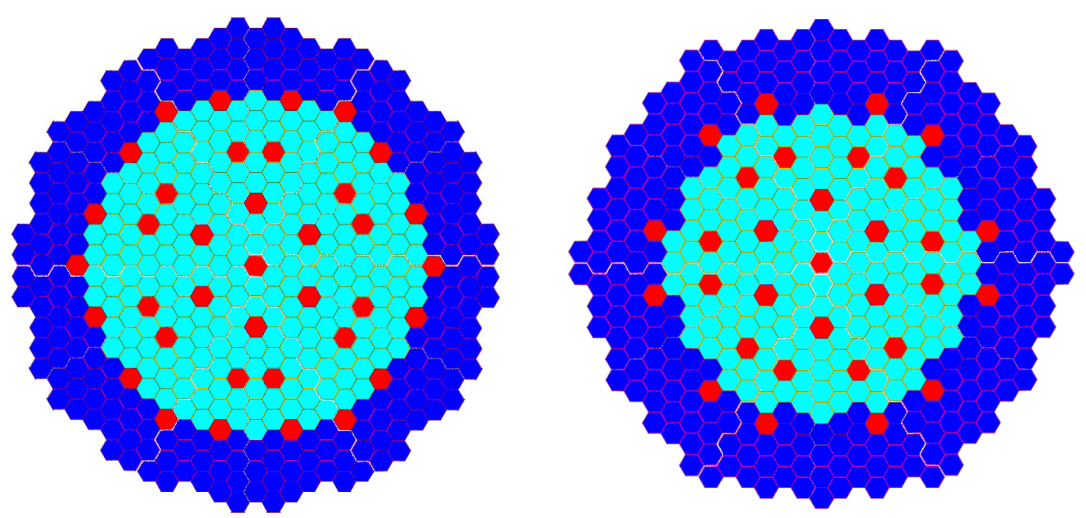


Figure 6 Cross-section of the COBRA models of oxide and carbide core of ESFR

## 3. Results

#### 3.1 Neutronic results

### 3.1.1 ESFR Oxide core

Neutronics safety parameters were evaluated using MCNP by the direct perturbation method. The reactivity coefficients, the delayed neutron fraction and the prompt neutron life time were calculated at different burnup stages. For the oxide core, the reactivity coefficients deteriorate over the fuel residence time whereas the variation in the delayed neutron fraction and prompt neutron life time is relatively low (Table 2).

Reactivity	BOL	EOC	
(pcm)			
Oxide core			
Sodium Void	1500	1968	
Doppler	-1044	-845	
$eta_{ m eff}$	338	320	

Table 2 Neutronic Safety Parameters O-SFR

The power distribution in initial oxide ESFR core is significantly determined by the two enrichment levels in the inner and outer core. At BOL, the power profile shows peak values in the outer core where

the fuel enrichment is high. The positioning of the primary CSD in this high power profile region may allow an effective power control. For the initial core at BOL, the core maximum power density is 354.83 W/cm<sup>3</sup>, and the peak of the axially averaged power density is 287.44 W/cm<sup>3</sup>. Further, the maximal linear power density is 408.16 W/cm and the power peak factor is 1.4. At EOC, the peak of the power profile is shifted inwards to the inner core. The power profile shows peak values in the inner core. The core maximum value is about 321.34 W/cm<sup>3</sup> and the peak of the axially averaged power density is 263.20 W/cm<sup>3</sup>. The maximal linear power density and the power peak factor are 373.44 W/cm and 1.21, respectively. The radial power peaking and distribution at BOL and EOC are shown in Figure 7 and Figure 8 respectively.

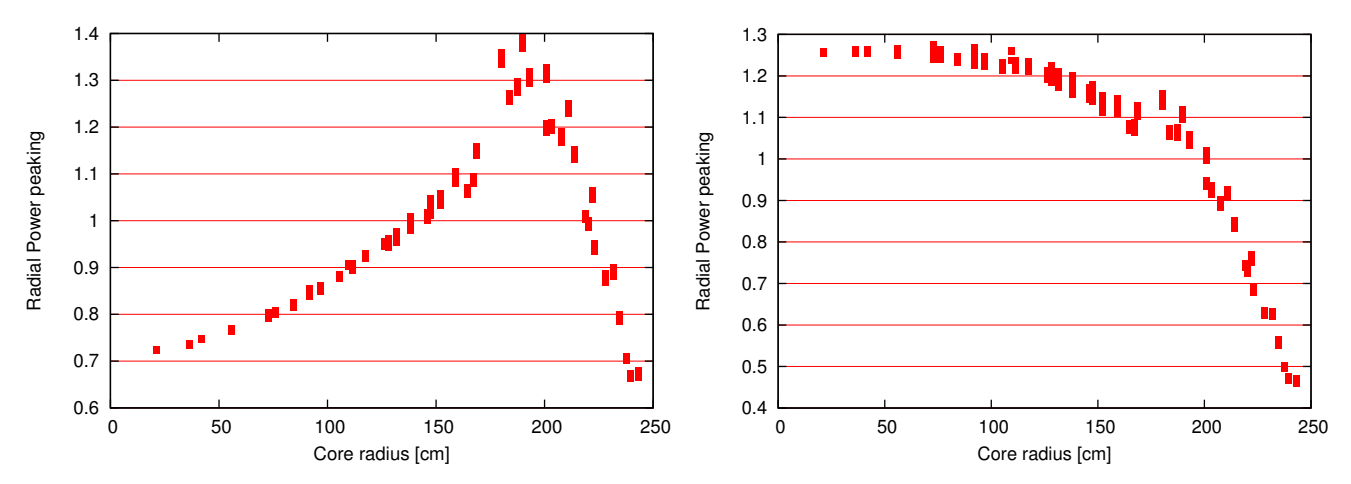


Figure 7 Radial power peaking of the oxide ESFR core at BOL and EOC

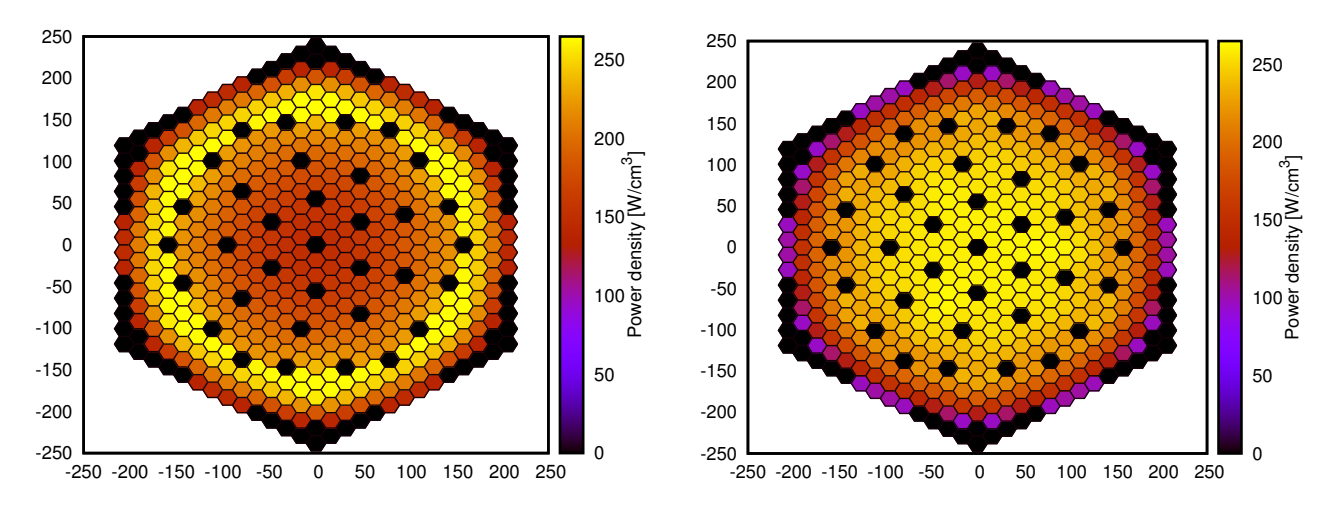


Figure 8 Average power distribution in the oxide ESFR core at BOL and EOC

#### 3.1.2 ESFR Carbide core

Like for the oxide core, the reactivity coefficients, the delayed neutron fraction and the prompt neutron life time for the carbide core have been evaluated using MCNP by direct perturbation calculations. Only the sodium void reactivity shows significant change over fuel residence time. The variation in the delayed neutron fraction and prompt neutron life time is relatively low (Table 3).

The power distribution in initial carbide ESFR core is characterized by the two enrichment levels in the inner and outer core. The power profile shows high values in the outer core where the fuel enrichment is high. The positioning of the primary CSD in this high power profile region may allow an effective power control. For the initial core at BOL, the core maximum power density is 681.55 W/cm3, and the peak of the axially averaged power density is 574.07 W/cm3. Further, the maximal linear power density is 504.1 W/cm and the power peak factor at BOL is 1.53.

Reactivity (pcm)	BOL	EOC
Carbide core		
Sodium Void	1131	1991
Doppler	-582	-648
$eta_{ m eff}$	349	319

Table 3 Neutronic Safety Parameters C-SFR

As the burnup progresses the power distribution keeps its profile and levels out only slightly. The core maximum value at EOC is about 531.32 W/cm3 and the peak of the axially averaged power density is 492.02 W/cm3. The maximal linear power density and the power peak factor are 432.05 W/cm and 1.31. The radial power peaking and distribution at BOL and EOC are shown in Figure 9 and Figure 10 respectively.

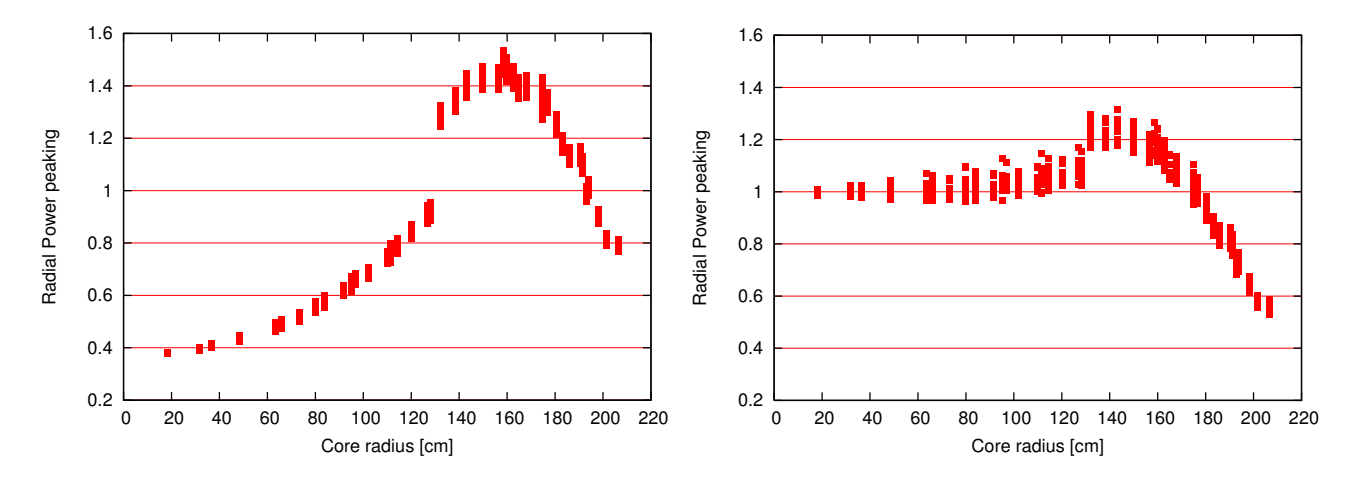


Figure 9 Radial power peaking of the carbide ESFR core at BOL and EOC

The 14<sup>th</sup> International Topical Meeting on Nuclear Reactor Thermalhydraulics, NURETH-14 Toronto, Ontario, Canada, September 25-30, 2011

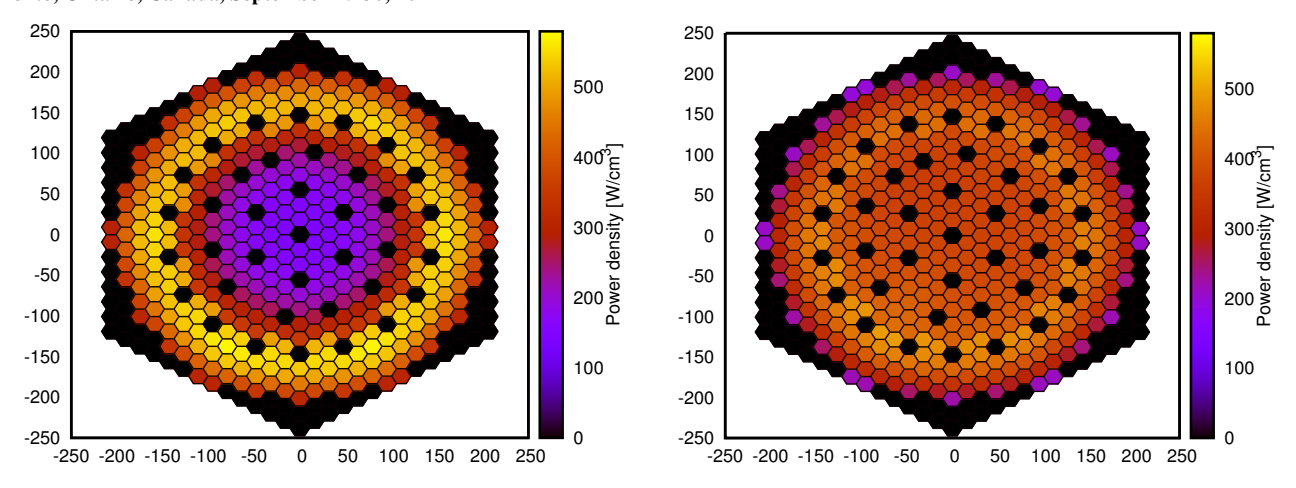


Figure 10 Average power distribution in the carbide ESFR core at BOL and EOC

## 3.2 Thermal-hydraulic results

The neutronics calculations (power distribution) provided the basis for the thermal-hydralic analysis. Calculations were performed for both the oxide and carbide core options (O-ESFR and C-ESFR) and included full core and sub-assembly studies.

The COBRA-IV-I thermal-hydraulic core and sub-channel code and the FRETA-B thermo-mechanic code, used for these simulations, were improved to account for the specificities of a liquid-metal cooled core. The Ushakov correlation [9] is adopted to calculate the clad-to-coolant heat exchange. The Rehme correlation [10] is used to evaluate the wire-wrapped fuel bundle friction factor.

## 3.2.1 ESFR oxide and carbide core

The total flowrate for all SAs to provide the heating-up of 150°C was found to be  $\sim$ 19550 kg/s and the corresponding flowrate for an average-power SA in oxide core is  $\sim$ 43 kg/swhile in carbide core is  $\sim$ 47 kg/s.

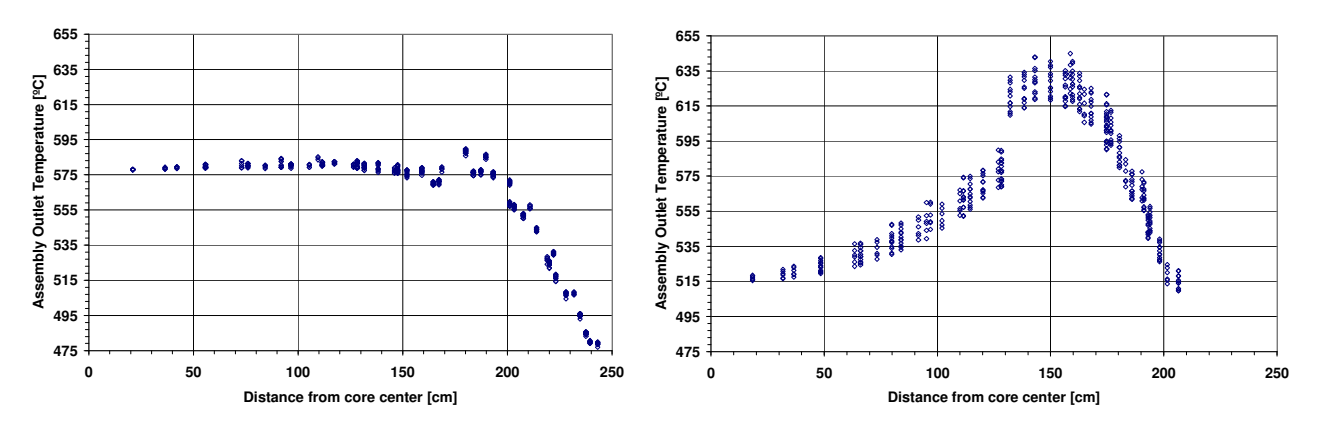


Figure 11 Outlet coolant temperature distribution in the oxide and carbide core

The coolant temperature at the core inlet was specified to be 395°C. The average outlet coolant temperature for both oxide and carbide cores was calculated to be ~545°C. The calculated outlet coolant temperature distribution is presented in Figure 11 and Figure 12.

The 14<sup>th</sup> International Topical Meeting on Nuclear Reactor Thermalhydraulics, NURETH-14 Toronto, Ontario, Canada, September 25-30, 2011

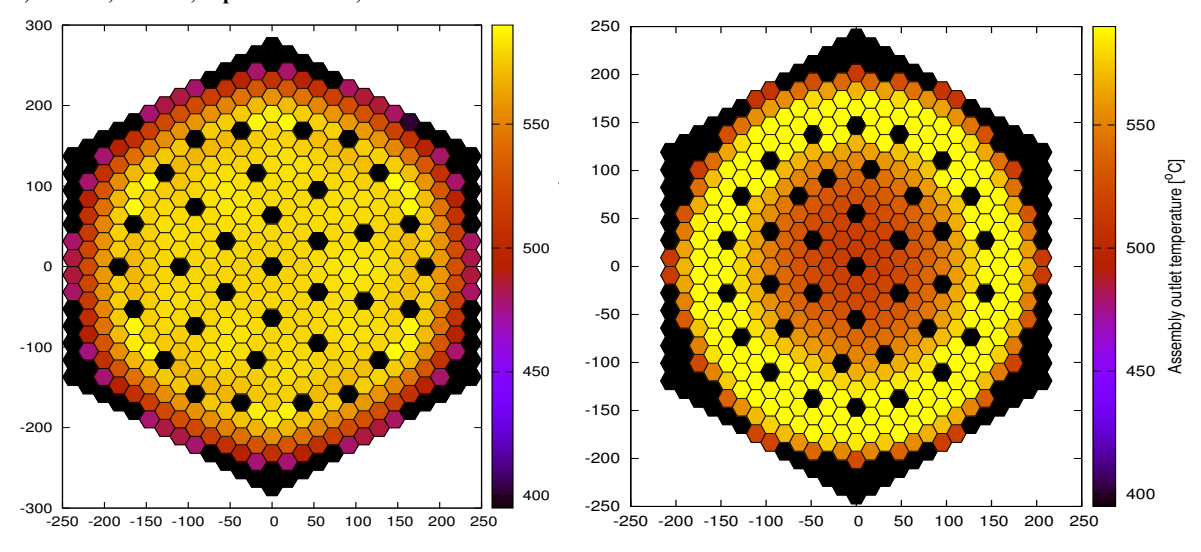


Figure 12 Outlet coolant temperature across the oxide and carbide core

As expected the coolant temperature profile is similar to the power distribution profile with a flat distribution in the centre of the core and a strong gradient at the core outskirts for the oxide core while higher temperatures are at three quarter of the carbide core. The difference between the maximum and minimum coolant temperature at the core outlet is about 110°C for the oxide and 120°C for the carbide core.

## 3.2.2 Fuel rod temperature

The fuel rod temperature was evaluated for the average- and peak-power fuel rods using the power distribution from neutronic analysis (axial and radial power peaking factors) and the coolant flowrate distribution from the thermal-hydraulic analysis.

As part of the ESAP, The FRETA-B code was used for this analysis. The ODS steel is supposed to be the ESFR cladding material.

The heat exchange coefficient was calculated by the Ushakov correlation, the fuel thermal conductivity was evaluated according to the Phillipponneau model [11] and the gas gap conductance was evaluated by the FRETA-B code using the Ross-Stoute model with the use of the modified fuel relocation model.

The axial profiles of the fuel, cladding and coolant temperatures in the average-power pin are shown in Figure 13. The fuel peak temperature in the oxide is ~1950°C while in the carbide average-power pin is ~1000 °C. The difference is due to the higher carbide conductivity ( $k_{(Pu,U)O2}$ =1.64 W/mK,  $k_{UC}$ =9.35 W/mK).

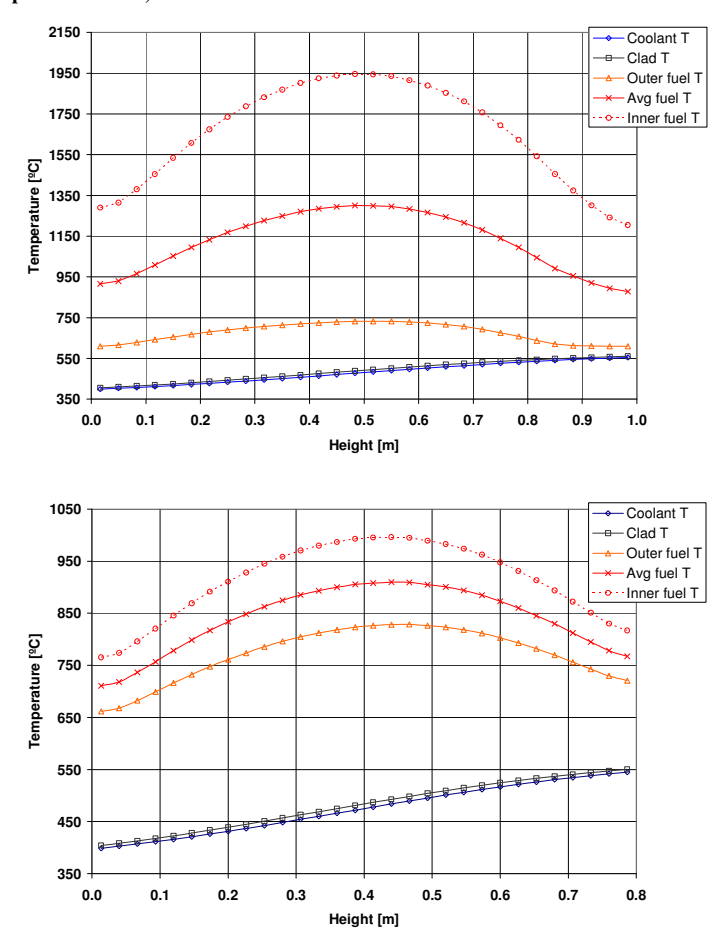


Figure 13 Axial temperature profiles in the oxide and carbide average-power pin

The total pressure drop is ~0.13 MPa in the oxide and ~0.20 MPa in the carbide assembly.

## 4. Conclusions

The European Safety Analysis Platform, being developed at JRC Institute of Energy, has the objective to develop a generic computational platform able to perform a static and dynamic integrated core and system safety analysis of nuclear reactors with particular emphasis to innovative concepts.

The static core design part of ESAP has been successfully applied in the framework of the FP7 CP-ESFR project. The results have shown the reliability of the platform to perform a full core design safety analysis with predictions that are in agreement with other consolidated code systems [12].

Though the results are still preliminary as they are based on the starting "working horses" core designs defined in the CP-ESFR project, some first conclusions can be made on the two core configurations.

In particular, while the oxide core design is quite mature, this seems not to be the case for the carbide core design. The advantages in using carbide fuel rely on a better fuel-sodium compatibility and thanks to the higher thermal conductivity ( $k_{(Pu,U)O2}$ =1.64 W/mK against  $k_{UC}$ =9.35 W/mK) on the possibility to have a de-rated design with a reduced power density (165 W/cm3), lower fuel centreline temperature, lower reactivity control requirement and longer cycle length enhancing safety. This is currently not the case in the current design, where the carbide core is still too compact to be fully exploited in this sense.

## The 14<sup>th</sup> International Topical Meeting on Nuclear Reactor Thermalhydraulics, NURETH-14 Toronto, Ontario, Canada, September 25-30, 2011

Future work will focus on the optimization of the different options with a view to enhance the core performance (average discharged burn-up, plutonium mass to be loaded, cycle length) and the safety by means of reduction of the sodium void coefficient and/or optimization leading to gain significant margins on the behaviour of these cores in the frame of unprotected transients.

## 5. References

- [1] A. Vasile, "The Collaborative Project for a European Sodium Fast Reactor CP ESFR", <u>Proceedings of the 11<sup>th</sup> International Congress on Advances in Nuclear Power Plants</u>, Nice, France, 2011 May 2-5.
- [2] R.E. MacFarlane and D.W. Muir, "The NJOY Nuclear Data Processing System, Version 91," Report LA-12740-M, October 1994
- [3] X-5 Monte-Carlo Team, "MCNP A General Monte Carlo N-Particle Transport Code, Version 5", Los Alamos National Laboratory, Tech. Report, 2003
- [4] J.S. Hendricks, "MCNPX 2.6.0 Manual", Los Alamos National Laboratory, Tech. Report, LA-CP-07-1473, April, 2008
- [5] C.L. Wheeler, C.W. Stewart, R.J. Cena, D.S. Rowe, A.M. Sutey, "COBRA-IV-I: an Interim Version of COBRA for Thermal-Hydraulic Analysis of Rod Bundles Nuclear Fuel Elements and Cores", 1976, BNWL-1962, Battelle, Pacific Northwest Laboratory, Richland, Washington.
- [6] M. Uchida, N. Otsubo, "Models of Multi-rod code FRETA-B for Transient Fuel Behaviour Analysis (Final Version)", 1984, JAERI 1293
- [7] W. B. Willson, "Recent development of CINDER'90 transmutation code and data library for actinides transmutation studies", GLOBAL'95 International Conference, Versailles, France, September 11-14
- [8] A.M. Ross and R.L. Stoute, "Heat Transfer Coefficient Between UO2 and Zircaloy-2", 1962. AECL-1552.
- [9] Mikityuk K. "Heat transfer to liquid metal: Review of data and correlations for tube bundles". Nuclear Engineering and Design 239 (2009) 680–687.
- [10] K. Rehme, "Pressure drop correlations for fuel element spacers.", 1973, Nuclear Technology.
- [11] Y. Philipponneau "Thermal conductivity of (U, Pu)O2-x mixed oxide fuel.", Journal of Nuclear Materials, Vol. 188, p.p. 194-197, 1992.
- [12] J. Krepel, K. Mikityuk, O. Huml, H. Tsige-Tamirat, L. Ammirabile, D. Blanchet, F. Polidoro, "Working horses ESFR core concepts characterization: neutronic and thermal-hydraulic characteristics", 2010, FP7 CP-ESFR project, deliverable SP2.1.2.D2